

LA-6360

c.3

CIC-14 REPORT COLLECTION
**REPRODUCTION
COPY**

UC-23

Reporting Date: May 1976

Issued: September 1976

**Numerical Simulation of Multiconstituent Diffusion and
Helium Release Characteristic of the $^{238}\text{PuO}_2$ Heat Source
Used in Radioisotopic Thermoelectric Generators**

by

Bruce D. McLaughlin



**Los Alamos
scientific laboratory**

of the University of California

LOS ALAMOS, NEW MEXICO 87545



An Affirmative Action/Equal Opportunity Employer

UNITED STATES
ENERGY RESEARCH AND DEVELOPMENT ADMINISTRATION
CONTRACT W-7405-ENG. 36

This work was supported by the Space Nuclear Systems.

Printed in the United States of America. Available from
National Technical Information Service
U.S. Department of Commerce
5285 Port Royal Road
Springfield, VA 22161
Price: Printed Copy \$4.00 Microfiche \$2.25

This report was prepared as an account of work sponsored by the United States Government. Neither the United States nor the United States Energy Research and Development Administration, nor any of their employees, nor any of their contractors, subcontractors, or their employees, makes any warranty, express or implied, or assumes any legal liability or responsibility for the accuracy, completeness, or usefulness of any information, apparatus, product, or process disclosed, or represents that its use would not infringe privately owned rights.

CONTENTS

LIST OF TABLES iv

LIST OF FIGURES iv

NOMENCLATURE iv

ABSTRACT 1

 I. INTRODUCTION 1

 II. MATHEMATICAL PRELIMINARIES 3

 III. ASSUMPTIONS 6

 A. Constituents 6

 B. Symmetry 6

 C. Singular Surfaces 7

 D. Body Force Densities 8

 E. Growth of Mass 8

 F. Stress 10

 G. Growth of Linear Momentum 11

 H. Heat Flow and Temperature 13

 IV. ANALYTICAL MODEL 15

 V. NUMERICAL INTEGRATION 18

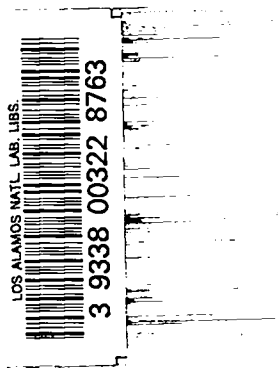
 VI. CONCLUSIONS AND DISCUSSION 18

 A. Helium 18

 B. Trace Impurity 19

 C. Plutonium-Uranium-Oxygen 21

REFERENCES 25



LIST OF TABLES

I.	CONSTITUENT AND GROUP IDENTIFICATIONS	7
II.	VALUES OF PLUTONIUM ISOTOPE DENSITIES AT $t = 0$	10
III.	TRACE IMPURITY CONTENT	20

LIST OF FIGURES

1.	Helium release.	19
2.	Computer-simulated radial density profile for calcium at 5 h.	21
3.	Computer-simulated radial density profile for calcium at 50 h.	21
4.	Computer-simulated radial density profile for calcium at 500 h.	22
5.	Computer-simulated radial density profile for calcium at 5000 h.	22
6.	Computer-simulated radial density profile for plutonium at 500 h.	23
7.	Computer-simulated radial density profile for uranium at 500 h.	23
8.	Computer-simulated radial density profile for oxygen at 500 h.	24

NOMENCLATURE

r_1^A	=	radius of heat source sphere at time zero
r_2^A	=	radius of spherical container
\bar{a}_r	=	the r^{th} group of constituents
\bar{B}_r	=	constitutive coefficient characteristic of \bar{a}_r
\bar{b}	=	body force per unit mass of mixture
\bar{b}_α	=	body force per unit mass of constituent α
\bar{b}_r	=	body force per unit mass of \bar{a}_r
$\bar{C}_{\alpha\beta}$	=	constitutive coefficient characteristic of constituents α and β
$\bar{C}_{r\ell}$	=	constitutive coefficient characteristic of \bar{a}_r and \bar{a}_ℓ
$\bar{D}_{\alpha\beta}$	=	constitutive coefficient characteristic of constituents α and β

$D^{r\ell}$	=	constitutive coefficient characteristic of $\overset{r}{a}$ and $\overset{\ell}{a}$
$\underline{d}^{r\ell}$	=	stretching tensor for constituent α
$\underline{d}^{r\ell\alpha}$	=	stretching tensor for $\overset{r}{a}$
$\langle \underline{d}^{r\ell\alpha} \rangle$	=	traceless part of $\underline{d}^{r\ell\alpha}$
$\langle \underline{d}^{r\ell} \rangle$	=	traceless part of $\underline{d}^{r\ell}$
$E^{\alpha\beta}$	=	constitutive coefficient characteristic of constituents α and β
$\underline{E}^{r\ell}$	=	constitutive coefficient characteristic of $\overset{r}{a}$ and $\overset{\ell}{a}$
e_i	=	covariant basis vector in spatial coordinates
$F^{\alpha\beta}$	=	constitutive coefficient characteristic of constituents α and β
$\underline{F}^{r\ell}$	=	constitutive coefficient characteristic of $\overset{r}{a}$ and $\overset{\ell}{a}$
$\underline{G}^{\alpha\beta}$	=	constitutive coefficient characteristic of constituents α and β
$\underline{G}^{r\ell}$	=	constitutive coefficient characteristic of $\overset{r}{a}$ and $\overset{\ell}{a}$
\underline{g}	=	metric tensor
\underline{H}^{α}	=	constitutive coefficient characteristic of constituent α
\underline{H}^r	=	constitutive coefficient characteristic of $\overset{r}{a}$
\underline{K}	=	thermal conductivity tensor
${}_1K$	=	thermal conductivity scalar in the $0 \leq R < {}_1A$ region
${}_2K$	=	thermal conductivity scalar in the ${}_1A < R$ region
${}^\alpha M$	=	atomic mass of constituent α
$\underline{m}^{\alpha r}$	=	group mass fraction of constituent α where $\overset{r}{a}$ contains α
${}^\alpha N$	=	atomic density of constituent α
\hat{n}	=	unit vector normal to a surface
n	=	number of constituents
\underline{n}	=	number of groups of constituents
\underline{p}^{α}	=	constitutive coefficient characteristic of constituent α
\underline{p}^r	=	constitutive coefficient characteristic of $\overset{r}{a}$
Q	=	body heating per unit volume of mixture per unit time (for $0 \leq R < {}_1A$)

- \bar{q} = heat flux for the mixture
- q^α = heat flux for constituent α
- $q^{\bar{a}}$ = heat flux for \bar{a}
- R = spherical coordinate measured along a radius
- $\underline{s}^{\alpha\beta}$ = mutual spin tensor for constituents α and β
- $\underline{s}^{\bar{a}\bar{b}}$ = mutual spin tensor for \bar{a} and \bar{b}
- s = body heating per unit mass of mixture per unit time
- s^α = body heating per unit mass of constituent α per unit time
- $s^{\bar{a}}$ = body heating per unit mass of \bar{a} per unit time
- \bar{T} = stress tensor for the mixture
- \underline{T}^α = stress tensor for constituent α
- $\underline{T}^{\bar{a}}$ = stress tensor for \bar{a}
- t = time
- u^i = spatial coordinate
- \bar{v} = velocity of the mixture
- v^α = velocity of constituent α
- $v^{\bar{a}}$ = velocity of \bar{a}
- \bar{W}^α = growth of linear momentum for constituent α
- χ^α = ρ^α at $t = 0$
- ϵ = energy per unit mass of mixture
- ϵ^α = energy per unit mass of constituent α
- $\epsilon^{\bar{a}}$ = energy per unit mass of \bar{a}
- θ = absolute temperature
- $\bar{\Lambda}$ = velocity of a discontinuity surface
- λ = $-\ln(1/2)/t_{1/2}$ where $t_{1/2}$ is the half-life of ^{238}Pu
- ρ = mass density of the mixture
- ρ^α = mass density of constituent α

$\bar{\rho}$	=	mass density of \bar{A}
Σ	=	a discontinuity surface
ω	=	growth of mass for constituent α
$\bar{\mathfrak{A}}$	=	growth of energy for constituent α
$\text{tr } \bar{d}^{\alpha}$	=	d^{α}_i or v^{α}_i
$\llbracket \quad \rrbracket$	=	jump of the quantity enclosed

Tensor components, not physical components, are used throughout.

A single bar above a letter indicates that the overall symbol denotes a first-order tensor.

A double bar above the letter indicates that the overall symbol denotes a second-order tensor.

Covariant differentiation with respect to u^j is indicated by the usual "j" subscript; e.g., $\partial \bar{v} / \partial u^j = v^i_{,j} e_i = v_{i,j} e^i$.

NUMERICAL SIMULATION OF MULTICONSTITUENT DIFFUSION AND HELIUM RELEASE
CHARACTERISTIC OF THE $^{238}\text{PuO}_2$ HEAT SOURCE USED IN
RADIOISOTOPIC THERMOELECTRIC GENERATORS

by

Bruce D. McLaughlin

ABSTRACT

This report describes an analytical model that was developed to simulate multiconstituent diffusion within a heat source sphere, helium generation within a heat source sphere, and helium release from the surface of a heat source sphere into the surrounding environment. This model represents the first attempt to simulate multiconstituent mass transport using the continuum thermomechanical theory of mixtures and demonstrates that this theory is a viable alternative to irreversible thermodynamics.

I. INTRODUCTION

A radioisotopic thermoelectric generator (RTG) derives its power from plutonium-oxide spheres. During manufacture, a heat source sphere consists of nominally stoichiometric plutonium oxide with various trace impurities. Six plutonium isotopes are present, with ^{238}Pu , ^{239}Pu , and ^{240}Pu accounting for more than 99% by weight. Radioactive decay of ^{238}Pu , by α emission, is responsible for the generation of helium within a heat source sphere and the generation of the heat itself. At the operating temperature of an RTG, the heat source is characterized by various mass transport phenomena. Within each individual sphere, trace impurities redistribute by means of thermal diffusion, sintering and associated densification can occur, helium is released from the sphere surface, and sublimation of trace impurities can occur. Because understanding these phenomena would be useful to the system designer, it is hoped that the work presented here constitutes a beginning toward the ultimate realization of a serviceable mass transport model.

The initial modeling effort covered only a small part of the overall mass transport problem, which includes (1) multiconstituent diffusion within a heat source sphere, (2) helium generation within a heat source sphere, and (3) helium release from the surface of a heat source sphere into the surrounding environment. Because this effort was only partially successful, the analytical model presented in this report should be regarded as a first-generation model. The model can adequately simulate helium generation and release, but it cannot adequately simulate the diffusion of all constituents of interest. The number of constituents should be increased by at least two, and explicit provisions should be made for using temperature-dependent constitutive coefficients.

My reasons for publishing this work, as opposed to waiting until the model was revised, are twofold. First, this model can adequately simulate helium generation and release. Second, it represents the first attempt to simulate multiconstituent mass transport using Truesdell's theory of mixtures. The partial success of this first-generation model demonstrates that this well-founded, but not widely used, theory is a viable alternative to nonequilibrium thermodynamics. For this theory to be accepted by the materials science community, there must be progress in certain areas associated with the theory (e.g., the experimental determination of constitutive coefficients). Possibly the work presented here will stimulate that progress.

The geometric-material system, on which the model is based, consists of a heat source sphere, with initial radius r_1A , placed concentrically inside a stationary spherical container of radius r_2A . The spherical container is presumed to be impermeable with regard to matter and permeable with regard to heat flux.

The first approach to solving the problem stated above was the straightforward application of Fick's Law $D\frac{\partial \rho}{\partial t} = \text{div}(D \text{ grad } \rho)$, where D represents diffusivity and D/Dt indicates the time derivative following the velocity of the mixture.¹ Unfortunately, certain assumptions, indigenous to Fick's Law, are incompatible with a heat source sphere. Fick's Law is obtained by substituting the constitutive relation $\rho(\frac{\partial}{\partial t} - \mathbf{v} \cdot \nabla) = -D \text{ grad } \rho$ into Eq. (1) and invoking the assumptions that the mixture is incompressible and the mass of constituent α is conserved. Furthermore, it is tacitly assumed that the mixture is binary. However, these restrictions are not insurmountable; modified versions of Fick's Law can be devised to accommodate compressibility, chemical and nuclear reactions, and more than two constituents. The two other tacit assumptions, which are also incompatible with a heat source sphere, are that the state of stress and the temperature

are constant throughout the mixture. These two assumptions cannot be removed by any straightforward process of accommodation. It was therefore concluded that Fick's Law is not an appropriate basis for developing an analytical model that characterizes a heat source sphere.

I also investigated the statistical-kinetic theory of diffusion, which is based on random walk analysis and the statistical theory of atomic jumps. Unfortunately, the basic irreversibility of mass transport in a temperature gradient is outside the scope of a quasi-equilibrium kinetic theory.²

This left, to my knowledge, two possible bases for developing the analytical model: (1) irreversible or nonequilibrium thermodynamics³ and (2) Truesdell's continuum thermomechanical theory of mixtures,⁴ which I ultimately chose.

To solve the balance equations, which are fundamental to Truesdell's theory of mixtures, several constitutive equations must be devised. My approach was guided by the following assumption: when the only processes taking place are multiconstituent diffusion, helium generation, and helium release, the heat source sphere behaves like a material that retains no memory of previous configurations. This assumption is presumed to be legitimate only if the sphere is not subjected to external loading and if the sphere has achieved a steady-state temperature distribution for a sufficient time to ensure the relaxation of all residual thermomechanical stresses.

A material that retains no memory of deformation history usually is called a fluid. To devise the constitutive equations, the heat source sphere was regarded as a mixture of fluids. The part of the geometric-material system outside the heat source sphere was also regarded as a mixture of fluids. Presumably, any material released from the heat source sphere becomes a gas where $1^A < R \leq 2^A$. This universal assumption of fluidity justified the use of Müller's constitutive equations⁵ for $\underline{\underline{T}}$ and $\underline{\underline{W}}$ throughout the geometric-material system.

II. MATHEMATICAL PRELIMINARIES

The balance equations, fundamental to the continuum thermomechanical theory of mixtures, are presented below. Refer to Refs. 4-7 for background information. Based on Truesdell's theory of mixtures, Eqs. (1)-(4) must be satisfied at each regular point of a mixture, and Eqs. (5)-(7) must be satisfied at each surface of discontinuity. Intrinsic surface properties, such as surface tension and surface production densities for mass, linear momentum, and energy, were ignored in the

derivations of Eqs. (1)-(7). Furthermore, it was assumed that the various constituents are nonmagnetic and nondielectric. It was also assumed that no couple stresses exist.

$$\frac{\partial \rho^\alpha}{\partial t} + \left(\frac{\alpha \alpha_i}{\rho v^i} \right)_{,i} = \rho \omega^\alpha . \quad (1)$$

$$\frac{\partial}{\partial t} \left(\frac{\alpha \alpha_i}{\rho v^i} \right) + \left(\frac{\alpha \alpha_i \alpha_j}{\rho v^i v^j} - \frac{\alpha_i j}{T} \right)_{,j} - \frac{\alpha \alpha_i}{\rho b^i} = \rho w^i . \quad (2)$$

$$\sum_{\alpha=1}^n \frac{\alpha_i j}{T} = \sum_{\alpha=1}^n \frac{\alpha_j i}{T} . \quad (3)$$

$$\frac{\partial}{\partial t} \left(\frac{\alpha \alpha}{\rho \epsilon} \right) + \left(\frac{\alpha \alpha \alpha_j}{\rho \epsilon v^j} - \frac{\alpha}{v^i} \frac{\alpha_i j}{T} - \frac{\alpha_j}{q} \right)_{,j} - \frac{\alpha \alpha}{\rho v^i} \frac{\alpha_i}{b^i} - \frac{\alpha \alpha}{\rho s} = \rho \Xi . \quad (4)$$

$$\left[\frac{\alpha}{\rho} \left(\frac{\alpha}{v} - \bar{\lambda} \right) \right] \cdot \hat{n} = 0 . \quad (5)$$

$$\left[\frac{\alpha \alpha_i}{\rho v^i} \left(\frac{\alpha_j}{v} - \lambda^j \right) - \frac{\alpha_i j}{T} \right] e_i e_j \cdot \hat{n} = \bar{0} . \quad (6)$$

$$\left[\frac{\alpha \alpha}{\rho \epsilon} \left(\frac{\alpha}{v} - \bar{\lambda} \right) - \frac{\alpha}{v} \cdot \frac{\alpha}{T} - \frac{\alpha}{q} \right] \cdot \hat{n} = 0 . \quad (7)$$

Quantities ω^α , w^i , and Ξ represent the production densities for mass, linear momentum, and energy, respectively. Exchanges of mass, linear momentum, and energy between constituents will not influence the mass, linear momentum, and energy of the total mixture. Therefore,

$$\sum_{\alpha=1}^n \omega^\alpha = 0, \quad \sum_{\alpha=1}^n w^i = \bar{0}, \quad \text{and} \quad \sum_{\alpha=1}^n \Xi = 0 . \quad (8)$$

The balance equations for the total mixture can be obtained from Eqs. (1)-(7) by using the following definitions.

$$\rho = \sum \rho^\alpha , \quad (9.1)$$

$$\rho v^i = \sum \frac{\alpha \alpha^i}{\rho v^i}, \quad (9.2)$$

$$\rho v^i v^j - T^{ij} = \sum \frac{\alpha \alpha^i \alpha^j}{\rho v^i v^j} - \sum \frac{\alpha^i \alpha^j}{T^{ij}}, \quad (9.3)$$

$$\rho b^i = \sum \frac{\alpha \alpha^i}{\rho b^i}, \quad (9.4)$$

$$\rho \epsilon v^j - v_i T^{ij} - q^j = \sum \frac{\alpha \alpha \alpha^j}{\rho \epsilon v^j} - \sum \frac{\alpha}{v_i} \frac{\alpha^i \alpha^j}{T^{ij}} - \sum \frac{\alpha^j}{q^j}, \quad (9.5)$$

$$\rho v_i b^i + \rho s = \sum \frac{\alpha \alpha}{\rho v_i b^i} + \sum \frac{\alpha \alpha}{\rho s}, \quad (9.6)$$

and

$$\rho \epsilon = \sum \frac{\alpha \alpha}{\rho \epsilon}. \quad (9.7)$$

In addition to viewing the mixture as an agglomeration of n constituents, view it also as a collection of \underline{n} groups of constituents, where $\underline{n} \leq n$ and the r^{th} group is denoted by \underline{r} . For all constituents α in \underline{r} , $\underline{v} = \underline{v}$, $\underline{b} = \underline{b}$, $\underline{\epsilon} = \underline{\epsilon}$, and $\underline{s} = \underline{s}$. Also,

$$\frac{\underline{r}}{\underline{\rho}} = \sum_{\alpha \text{ in } \underline{r}} \frac{\alpha}{\underline{\rho}}, \quad \frac{\underline{r}}{\underline{T}} = \sum_{\alpha \text{ in } \underline{r}} \frac{\alpha}{\underline{T}}, \quad \text{and} \quad \frac{\underline{r}}{\underline{q}} = \sum_{\alpha \text{ in } \underline{r}} \frac{\alpha}{\underline{q}}. \quad (10)$$

Using these newly defined group quantities, the balance equations for a group of constituents can be obtained from Eqs. (1)-(7).

$$\frac{\underline{r}}{\underline{\rho}} \frac{\partial \underline{\rho}}{\partial t} + \left(\frac{\underline{r} \underline{r} i}{\underline{\rho} \underline{v}^i} \right)_{,i} = \sum_{\alpha \text{ in } \underline{r}} \frac{\alpha}{\underline{\rho} \underline{\omega}}. \quad (11)$$

$$\frac{\partial}{\partial t} \left(\frac{\underline{r} \underline{r} i}{\underline{\rho} \underline{v}^i} \right) + \left(\frac{\underline{r} \underline{r} i \underline{r} j}{\underline{\rho} \underline{v}^i \underline{v}^j} - \frac{\underline{r} \underline{r} i j}{\underline{T}^{ij}} \right)_{,j} - \frac{\underline{r} \underline{r} i}{\underline{\rho} \underline{b}^i} = \sum_{\alpha \text{ in } \underline{r}} \frac{\alpha^i}{\underline{\rho} \underline{w}^i}. \quad (12)$$

$$\sum_{r=1}^{\underline{n}} \frac{\underline{r}}{\underline{T}^{ij}} i j = \sum_{r=1}^{\underline{n}} \frac{\underline{r}}{\underline{T}^{ji}} j i. \quad (13)$$

$$\frac{\partial}{\partial t} \left(\frac{\underline{r} \underline{r}}{\underline{\rho} \underline{\epsilon}} \right) + \left(\frac{\underline{r} \underline{r} \underline{r} j}{\underline{\rho} \underline{\epsilon} \underline{v}^j} - \frac{\underline{r}}{\underline{v}_i} \frac{\underline{r} \underline{r} i j}{\underline{T}^{ij}} - \frac{\underline{r} j}{\underline{q}^j} \right)_{,j} - \frac{\underline{r} \underline{r}}{\underline{\rho} \underline{v}_i \underline{b}^i} - \frac{\underline{r} \underline{r}}{\underline{\rho} \underline{s}} = \sum_{\alpha \text{ in } \underline{r}} \frac{\alpha}{\underline{\rho} \underline{s}}. \quad (14)$$

$$\left[\left[\frac{r}{\rho} \left(\frac{r}{v} - \bar{\lambda} \right) \right] \right] \cdot \hat{n} = 0 \quad (15)$$

$$\left[\left[\frac{r r_i}{\rho v} \left(\frac{r_j}{v} - \lambda^j \right) - \frac{r_{ij}}{T} \right] \right] e_i e_j \cdot \hat{n} = \bar{0} \quad (16)$$

$$\left[\left[\frac{r r}{\rho \epsilon} \left(\frac{r}{v} - \bar{\lambda} \right) - \frac{r}{v} \cdot \frac{r}{T} - \frac{r}{q} \right] \right] \cdot \hat{n} = 0 \quad (17)$$

When it does not seem reasonable to view a group of constituents as one constituent from the very beginning, use Eqs. (11)-(17) instead of Eqs. (1)-(7) to reduce the number of equations to be solved. One useful characteristic of a group of constituents is that the group mass fractions, defined by

$$\underline{\alpha}_m^r = \frac{\alpha^r}{\rho/\rho}, \quad \text{where } \overset{r}{\alpha} \text{ contains } \alpha, \quad (18)$$

are unaffected by the motion of the mixture. In other words, the $\underline{\alpha}_m^r$ are, at most, functions of time and can always be determined from a stationary reference configuration.

III. ASSUMPTIONS

A. Constituents

Development of the analytical model and generation of the experimental data for comparison were done simultaneously. Consequently, the selection of constituents was based as much on intuition as on fact. All six plutonium isotopes were included as constituents with the element plutonium representing a group. Oxygen was selected as an individual constituent, instead of being attached to the plutonium isotope constituents, because the heat source material is slightly hypostoichiometric with respect to oxygen even under constant temperature and state of stress throughout. Uranium-234 and helium were selected as constituents because of the decomposition reaction $^{238}\text{Pu} \rightarrow ^{234}\text{U} + ^4\text{He}$. Finally, a constituent called "trace impurity" was included to account for species such as aluminum, silicon, and calcium, which are present in concentrations from 50 to 500 ppm. Individual constituents and groups of constituents are listed in Table I.

B. Symmetry

It was assumed that the geometric-material system is characterized by spherical symmetry throughout its lifetime. Therefore, if a spherical, curvilinear, coordinate system is used, where $u^1 = R$ is the radial coordinate, then

TABLE I

CONSTITUENT AND GROUP IDENTIFICATIONS

Constituent	^{236}Pu	^{238}Pu	^{239}Pu	^{240}Pu	^{241}Pu	^{242}Pu	^{234}U	Helium	Oxygen	Trace Impurity
α	1	2	3	4	5	6	7	8	9	10
\bar{r}	$\bar{1}$	$\bar{2}$	$\bar{3}$	$\bar{4}$	$\bar{5}$	$\bar{6}$	$\bar{7}$	$\bar{8}$	$\bar{9}$	$\bar{10}$
\bar{a}	\bar{a}	\bar{a}	\bar{a}	\bar{a}	\bar{a}	\bar{a}	\bar{a}	\bar{a}	\bar{a}	\bar{a}

- (a) any scalar, vector, or second-order tensor quantity, which is generally functionally dependent on u^i and t , can be expressed as a function of R and t ; and
- (b) the only possible nonzero component of $\bar{\phi}$ is $\bar{\phi}^1 = \phi_1 = \phi$, where $\bar{\phi}$ represents \bar{v} , \bar{v} , \bar{v} , \bar{b} , \bar{b} , \bar{b} , \bar{q} , \bar{q} , \bar{q} , $\bar{\lambda}$, and \bar{W} .

C. Singular Surfaces

As mentioned in Sec. I, the analytical model was developed to represent a geometric-material system that consisted of a heat source sphere placed concentrically inside a fixed, impermeable spherical container. During development we assumed that the only singular surface in this geometric-material system was the $R = \frac{1}{2}A$ surface. Consequently, many discontinuity surfaces, characteristic of a real heat source sphere, were ignored. Examples of such surfaces are grain boundaries, surfaces created by agglomeration of vacancies, surfaces created by the formation of helium bubbles, and pore surfaces, which are created in the heat source sphere during the sintering process. Although some of these "ignored" singular surfaces may have a significant influence on the mass transport characteristics of a heat source sphere, the simulation of that influence is beyond the capabilities of this first-generation model.

The justification for assuming that the stationary surface $R = \frac{1}{2}A$ is a singular surface for all t is that at $t = 0$ there is a physically discernible surface at $R = \frac{1}{2}A$. This surface is singular with respect to $\bar{\rho}$, $\bar{\rho}$, and $\bar{\rho}$ and is probably singular with respect to $\text{grad } \theta$.

When $t > 0$, one would still expect to find a physically discernible surface at $R = \frac{1}{2}A$, although multiconstituent diffusion and helium generation have occurred where $0 \leq R < \frac{1}{2}A$ and helium has moved across the surface from the region $0 \leq R < \frac{1}{2}A$ to the region $\frac{1}{2}A < R \leq A$. Where $t > 0$, this surface might be singular with respect to all $\bar{\rho}$, \bar{v} , \bar{I} , \bar{q} , $\bar{\epsilon}$ and their derivatives. Consequently, it did not seem reasonable to assume that the jump equations are automatically satisfied at $R = \frac{1}{2}A$ (henceforth denoted by Σ).

$\bar{\lambda} = \bar{0}$ because Σ is stationary, and $\hat{n} = e_1 = e^1$ because Σ is a sphere. Using the assumption of spherical symmetry, Eqs. (15) and (16) become

$$\left[\left[\begin{array}{c} r \\ \rho v \end{array} \right] \right] = 0, \quad (19)$$

$$\left[\left[\begin{array}{c} r \\ \rho \end{array} \left(\frac{r}{v} \right)^2 - \bar{T}^{11} \right] \right] = 0, \quad (20)$$

$$\left[\left[\begin{array}{c} r \\ \bar{T} \end{array} \right]^{21} \right] = 0, \quad (21)$$

and

$$\left[\left[\begin{array}{c} r \\ \bar{T} \end{array} \right]^{31} \right] = 0. \quad (22)$$

Equations (7) or (17) cannot be used without a constitutive equation for \bar{q}^α . Such an equation would contain a thermal conductivity, which is characteristic of constituent α and may differ from the thermal conductivity of the mixture. Because thermal conductivities for individual constituents have not been defined adequately, we used the following approach to avoid using such parameters. Equation (7) was summed over all α to yield

$$\left[\left[\rho \epsilon (\bar{v} - \bar{\lambda}) - \bar{v} \cdot \bar{T} - \bar{q} \right] \right] \cdot \hat{n} = 0. \quad (23)$$

We then assumed that the energy flow, attributable to mass transport (convection), is insignificant when compared with heat flux (conduction). Therefore, Eq. (23) reduces to $\left[\left[\bar{q} \right] \right] \cdot \hat{n} = 0$ or

$$\left[\left[q \right] \right] = 0. \quad (24)$$

In other words, we assumed that q is continuous across Σ .

D. Body Force Densities

It was assumed that $\bar{b} = \bar{0}$ for all constituents α .

E. Growth of Mass

Because ^{239}Pu and ^{240}Pu possess half-lives of 24 300 and 6 600 yr, respectively, they were viewed as stable isotopes. Further, ^{236}Pu , ^{241}Pu , and ^{242}Pu are present in such small quantities that they were viewed as unchanging, although the ^{236}Pu and ^{241}Pu half-lives are smaller than the ^{238}Pu half-life. The only reaction considered, during development of the model, was the nuclear decomposition reaction $^{238}\text{Pu} \rightarrow ^{234}\text{U} + ^4\text{He}$.

Let N^α represent the atomic density of constituent α . By definition, $\rho^\alpha = \frac{N^\alpha}{M}$ where M is the atomic mass of constituent α and is presumed to be constant. Now consider a hypothetical situation in which the nuclear decomposition reaction ${}^{238}\text{Pu} \rightarrow {}^{234}\text{U} + {}^4\text{He}$ is allowed to take place but all constituent velocities are constrained to zero ($\vec{v}^\alpha = \vec{0}$ for all α). Under such conditions $\frac{\partial N^\alpha}{\partial t} = 0$ for $\alpha = 1, 3, 4, 5, 6, 9, 10$, and $\frac{\partial N^\alpha}{\partial t} = -\lambda N^\alpha$ for $\alpha = 2, 7, 8$. The constituents, referred to by number, are identified in Table I, and $\lambda = -\ln(1/2)/t_{1/2}$ where $t_{1/2} = 87.8$ yr so that $\lambda = 2.51 \times 10^{-10} \text{ s}^{-1}$.

We obtained ρ^α by determining $\frac{\partial \rho^\alpha}{\partial t}$ when all constituent velocities are constrained to zero. Under such conditions $\frac{\partial \rho^\alpha}{\partial t} = \frac{\partial}{\partial t} \left(\frac{N^\alpha}{M} \right)$. It follows that $\rho^\alpha = 0$ for $\alpha = 1, 3, 4, 5, 6, 9$, and 10 ; $\rho^2 = -\lambda \rho^2$; $\rho^7 = \lambda \rho^7 M/M$; and $\rho^8 = \lambda \rho^8 M/M$. Summing the expressions for ρ^α over all α in \vec{a} yields

$$\sum_{\alpha \text{ in } \vec{a}} \rho^\alpha = -\lambda \frac{21}{m} \frac{1}{\rho},$$

$$\sum_{\alpha \text{ in } \vec{a}} \rho^\alpha = \frac{234}{238} \lambda \frac{21}{m} \frac{1}{\rho},$$

$$\sum_{\alpha \text{ in } \vec{a}} \rho^\alpha = \frac{4}{238} \lambda \frac{21}{m} \frac{1}{\rho}$$

(25)

and

$$\sum_{\alpha \text{ in } \vec{a}} \rho^\alpha = \sum_{\alpha \text{ in } \vec{a}} \rho^\alpha = 0.$$

Here we derive expressions for the various $\frac{\alpha r}{m}$. Note that $\frac{21}{m}$ is needed for Eq. (25) and that all the $\frac{\alpha r}{m}$ are contained in Eq. (31), which defines linear momentum growth for a group. Obviously $\frac{72}{m} = \frac{83}{m} = \frac{94}{m} = \frac{105}{m} = 1$ because each of the \vec{a} , \vec{a} , \vec{a} , and \vec{a} groups comprises one constituent. To determine the remaining six $\frac{\alpha r}{m}$, recall that the $\frac{\alpha r}{m}$ are unaffected by the motion of the mixture and thus can be determined from a reference configuration where all \vec{v}^α are constrained to $\vec{0}$. Under such conditions $\frac{\partial \rho^\alpha}{\partial t} = 0$ for $\alpha = 1, 3, 4, 5$, and 6 and $\frac{\partial \rho^\alpha}{\partial t} = -\lambda \rho^\alpha$. Integration yields $\rho^\alpha = \chi^\alpha$ for $\alpha = 1, 3, 4, 5$, and 6 , and $\rho^2 = \chi^2 e^{-\lambda t}$ where the various χ^α are, at most, functions of spatial position (u^i). It follows that

$$\frac{\rho_{21}}{\rho} = \frac{\rho_0^2 \chi e^{-\lambda t}}{\rho_0 \chi e^{-\lambda t} + \sum_{\alpha=1,3,4,5,6} \rho_0^\alpha \chi}$$

and

(26)

$$\frac{\rho_{\alpha 1}}{\rho} = \frac{\rho_0^\alpha \chi}{\rho_0 \chi e^{-\lambda t} + \sum_{\alpha=1,3,4,5,6} \rho_0^\alpha \chi} \quad \alpha = 1, 3, 4, 5, \text{ and } 6.$$

The χ represents ρ^α at $t = 0$; that is, $\chi = \rho^\alpha (u^i, 0)$. At $t = 0$ it is reasonable, but not necessary, to assume that plutonium is distributed uniformly throughout a heat source sphere. This assumption implies that the χ are constants. The experimentally determined "typical" values used are given in Table II.

F. Stress

Generalizing Müller's expression for $\frac{\rho}{T}$, to an arbitrary number of constituents, yields⁵

$$\frac{\rho}{T} = \left[-\frac{\rho}{P} + \sum_{\beta=1}^n \frac{\rho^{\alpha\beta}}{C} \left(\text{tr} \frac{\beta}{d} \right) \right] \bar{g} + \sum_{\beta=1}^n 2 \frac{\rho^{\alpha\beta}}{D} \left\langle \frac{\beta}{d} \right\rangle - \sum_{\beta=1}^n \frac{\rho^{\alpha\beta} \rho^{\alpha\beta}}{E S}, \quad (27)$$

where

$$\frac{\beta}{d}_{ij} = \frac{1}{2} (v_{i,j}^\beta + v_{j,i}^\beta) \quad \text{and} \quad s_{ij}^{\alpha\beta} = \frac{1}{2} (v_{i,j}^\alpha - v_{j,i}^\alpha) - \frac{1}{2} (v_{i,j}^\beta - v_{j,i}^\beta).$$

TABLE II

VALUES OF PLUTONIUM ISOTOPE DENSITIES AT $t = 0$

Constituent	^{236}Pu	^{238}Pu	^{239}Pu	^{240}Pu	^{241}Pu	^{242}Pu
α	1	2	3	4	5	6
ρ^α χ (kg/m ³)	0.012	8112	1609	306	66	14

Summing Eq. (27) over all α in \underline{a} yields

$$\underline{\underline{T}}^r = \left[-\underline{\underline{P}}^r + \sum_{\ell=1}^n \underline{\underline{C}}^{r\ell} \left(\text{tr} \underline{\underline{d}}^{\ell} \right) \right] \underline{\underline{g}} + \sum_{\ell=1}^n \frac{r\ell}{2\underline{\underline{D}}} \langle \underline{\underline{d}}^{\ell} \rangle - \sum_{\ell=1}^n \frac{r\ell r\ell}{\underline{\underline{E}} \underline{\underline{s}}}, \quad (28)$$

where

$$\underline{\underline{P}}^r = \sum_{\alpha} \sum_{\text{in } \underline{a}} \underline{\underline{P}}^{\alpha}, \quad \underline{\underline{C}}^{r\ell} = \sum_{\alpha} \sum_{\text{in } \underline{a}} \sum_{\beta} \sum_{\text{in } \underline{a}}^{\ell} \alpha\beta \underline{\underline{C}}^{r\ell}, \quad \underline{\underline{D}} = \sum_{\alpha} \sum_{\text{in } \underline{a}} \sum_{\beta} \sum_{\text{in } \underline{a}}^{\ell} \alpha\beta \underline{\underline{D}}, \quad \text{and} \quad \underline{\underline{E}} = \sum_{\alpha} \sum_{\text{in } \underline{a}} \sum_{\beta} \sum_{\text{in } \underline{a}}^{\ell} \alpha\beta \underline{\underline{E}}.$$

By definition, $\langle \underline{\underline{d}}^{\ell} \rangle = \underline{\underline{d}}^{\ell} - (1/3) (\text{tr} \underline{\underline{d}}^{\ell}) \underline{\underline{g}}$. The assumption of spherical symmetry implies that $\underline{\underline{s}}^{\ell} = \underline{\underline{0}}$ and $\text{tr} \underline{\underline{d}}^{\ell} = \underline{\underline{d}}^{\ell} = [1/R^2] [\partial(R^2 \underline{\underline{v}}^{\ell}) / \partial R]$ and that the only nonzero, double contravariant components of $\underline{\underline{d}}^{\ell}$ are $\underline{\underline{d}}^{\ell 11} = \partial \underline{\underline{v}}^{\ell} / \partial R$, $\underline{\underline{d}}^{\ell 22} = \underline{\underline{v}}^{\ell} g^{22} / R$, and $\underline{\underline{d}}^{\ell 33} = \underline{\underline{v}}^{\ell} g^{33} / R$. Letting $\underline{\underline{P}}^r = \underline{\underline{B}}_0 \theta^r$, it follows that $\underline{\underline{T}}^{ij} = 0$ for $i \neq j$ and

$$\begin{aligned} \underline{\underline{T}}^{11} &= \left[-\underline{\underline{B}}_0 \theta^r + \frac{1}{R^2} \sum_{\ell=1}^n \left(\underline{\underline{C}}^{r\ell} - \frac{2}{3} \underline{\underline{D}}^{r\ell} \right) \frac{\partial}{\partial R} \left(R^2 \underline{\underline{v}}^{\ell} \right) \right] + \sum_{\ell=1}^n \frac{r\ell}{2 \underline{\underline{D}}} \frac{\partial \underline{\underline{v}}^{\ell}}{\partial R}, \\ \underline{\underline{T}}^{22} &= \left[-\underline{\underline{B}}_0 \theta^r + \frac{1}{R^2} \sum_{\ell=1}^n \left(\underline{\underline{C}}^{r\ell} - \frac{2}{3} \underline{\underline{D}}^{r\ell} \right) \frac{\partial}{\partial R} \left(R^2 \underline{\underline{v}}^{\ell} \right) \right] g^{22} + \sum_{\ell=1}^n \frac{r\ell}{2 \underline{\underline{D}}} \frac{\underline{\underline{v}}^{\ell} g^{22}}{R}, \end{aligned} \quad (29)$$

and

$$\underline{\underline{T}}^{33} = \underline{\underline{T}}^{22} \frac{g^{33}}{g^{22}}.$$

G. Growth of Linear Momentum

Generalizing Miller's expression for $\underline{\underline{W}}^{\alpha}$, to an arbitrary number of constituents, yields⁵

$$\underline{\underline{W}}^{\alpha} = - \sum_{\beta=1}^n \alpha\beta \underline{\underline{F}}^{\alpha\beta} \left(\frac{\alpha}{v} - \frac{\beta}{v} \right) - \sum_{\beta=1}^n \frac{\alpha\beta}{\underline{\underline{G}}} \underline{\underline{G}} \cdot \text{grad } \rho^{\beta} - \underline{\underline{H}} \cdot \text{grad } \theta. \quad (30)$$

Summing Eq. (30) over all α in \bar{a} yields

$$\sum_{\alpha \text{ in } \bar{a}} \underline{\underline{W}}^{\alpha} = - \sum_{\ell=1}^n \underline{\underline{F}}^{\ell} \left(\underline{\underline{v}}^{\ell} - \underline{\underline{v}} \right) - \sum_{\ell=1}^n \underline{\underline{G}}^{\ell} \cdot \text{grad } \underline{\underline{\rho}} - \underline{\underline{H}} \cdot \text{grad } \theta, \quad (31)$$

where

$$\underline{\underline{F}}^{\ell} = \sum_{\alpha \text{ in } \bar{a}} \sum_{\beta \text{ in } \bar{a}} \underline{\underline{F}}^{\alpha\beta} \underline{\underline{r}}^{\ell}, \quad \underline{\underline{G}}^{\ell} = \sum_{\alpha \text{ in } \bar{a}} \sum_{\beta \text{ in } \bar{a}} \underline{\underline{G}}^{\alpha\beta} \underline{\underline{m}}^{\beta\ell}, \quad \text{and } \underline{\underline{H}} = \sum_{\alpha \text{ in } \bar{a}} \underline{\underline{H}}^{\alpha}.$$

Because $\sum_{\alpha} \underline{\underline{W}}^{\alpha} = \bar{0}$, we have the following restrictions on the constitutive coefficients in Eq. (31).

$$\sum_{r=1}^n \left(\underline{\underline{F}}^{r\ell} - \underline{\underline{F}}^{\ell r} \right) = 0, \quad \sum_{r=1}^n \underline{\underline{G}}^{r\ell} = \bar{0}, \quad \text{and } \sum_{r=1}^n \underline{\underline{H}}^r = \bar{0}. \quad (32)$$

By assuming that the geometric-material system is characterized by thermal and material isotropy, we obtain $\underline{\underline{G}}^{r\ell} = \underline{\underline{G}}^{\ell r}$ and $\underline{\underline{H}} = \underline{\underline{H}}^g$. Using the assumption of spherical symmetry, we obtain $\sum_{\alpha \text{ in } \bar{a}} \underline{\underline{W}}^{\alpha 2} = \sum_{\alpha \text{ in } \bar{a}} \underline{\underline{W}}^{\alpha 3} = 0$ and

$$\sum_{\alpha \text{ in } \bar{a}} \underline{\underline{r}}^{\alpha} \rho \underline{\underline{W}}^{\alpha} = -\rho \sum_{\ell=1}^n \underline{\underline{F}}^{\ell} \left(\underline{\underline{v}}^{\ell} - \underline{\underline{v}} \right) - \rho \sum_{\ell=1}^n \underline{\underline{G}}^{\ell} \frac{\partial \rho}{\partial R} - \rho \underline{\underline{H}} \frac{\partial \theta}{\partial R}. \quad (33)$$

According to constitutive theory,⁵ coefficients such as $\underline{\underline{F}}^{\ell}$, $\underline{\underline{G}}^{\ell}$, and $\underline{\underline{H}}$ should be time independent. If $\underline{\underline{F}}$ and $\underline{\underline{H}}$ are time independent, then $\underline{\underline{F}}^{\ell}$ and $\underline{\underline{H}}^{\alpha}$ are also time independent. However, the $\underline{\underline{m}}^{\beta\ell}$ generally are functions of time, Eq. (26), and it would appear that this time dependence should be transferred to $\underline{\underline{G}}^{\ell}$. This inconsistency can be removed by assuming that the $\underline{\underline{G}}^{\alpha\beta}$ are identical for all β in a given group; therefore,

$$\underline{\underline{G}}^{\ell} = \sum_{\alpha \text{ in } \bar{a}} \sum_{\beta \text{ in } \bar{a}} \underline{\underline{G}}^{\alpha\beta} \underline{\underline{m}}^{\beta\ell} = \sum_{\alpha \text{ in } \bar{a}} \underline{\underline{G}}^{\alpha\ell} \sum_{\beta \text{ in } \bar{a}} \underline{\underline{m}}^{\beta\ell} = \sum_{\alpha \text{ in } \bar{a}} \underline{\underline{G}}^{\alpha\ell}. \quad (34)$$

and the \underline{m} time dependence is removed from \underline{G} .

When $r = \ell$, it can be assumed that $\underline{F}^{\underline{r}\underline{\ell}} = 0$ with no loss of generality. Thus, there are $\underline{n}(\underline{n}-1)$ possible nonvanishing \underline{F} , which are constrained by the \underline{n} linear equations $\sum_{r=1}^{\underline{n}} (\underline{F}^{\underline{r}\underline{\ell}} - \underline{F}^{\underline{\ell}r}) = 0$ of which only $\underline{n}-1$ are independent.¹ Therefore, the maximum number of independent nonvanishing \underline{F} is $(\underline{n}-1)^2$. During development of the model, we assumed that $\underline{F}^{\underline{r}\underline{\ell}} = \underline{F}^{\underline{\ell}r}$. This assumption provides $(1/2)\underline{n}(\underline{n}-1)$ independent linear equations and reduces the maximum number of independent nonvanishing coefficients to $(1/2)\underline{n}(\underline{n}-1)$.

Note that Eq. (30) does not contain either a nuclear decomposition or a chemical reaction contribution, which would presumably have the form $\omega^{\alpha} \bar{v}^{\alpha}$, where \bar{v}^{α} is the mean velocity of newly created, or destroyed, α mass. Ignoring the $\omega^{\alpha} \bar{v}^{\alpha}$ to \bar{W} contribution is equivalent to assuming that either $\omega^{\alpha} = 0$ or $\bar{v}^{\alpha} = \bar{0}$. Because the reaction ${}_{2}^{238}\text{Pu} \rightarrow {}_{7}^{234}\text{U} + {}_{8}^{4}\text{He}$ is occurring throughout the heat source sphere, we cannot assume that ω , ω , and ω can be approximated by zero. Such an assumption would, in fact, be inconsistent with Eq. (25). However, we did assume that $\bar{v}^{\alpha} = \bar{v}^{\alpha} = \bar{v}^{\alpha} = \bar{0}$. Because \bar{v}^{α} represents a mean velocity, this would seem to be a reasonable assumption for all regions except those near the surface Σ . It is hoped that deviations from $\bar{v}^{\alpha} = \bar{0}$, near Σ , are of insufficient magnitude to invalidate the use of Eq. (30).

H. Heat Flow and Temperature

Summing Eq. (4) over all α yields

$$\frac{\partial}{\partial t} (\rho \epsilon) + (\rho \epsilon v^j - v_i T^{ij} - q^j)_{,j} - \rho v_i b^i - \rho s = 0, \quad (35)$$

which represents the equation of energy balance for the mixture. Recalling the assumptions that

(a) $b^i = 0$ and

(b) the flow of energy, due to mass transport, is insignificant compared with heat flux,

and introducing the new assumptions that

(c) steady state has been achieved with regard to energy flow and

(d) $\bar{q} = \bar{K} \cdot \text{grad} \theta$,

causes Eq. (35) to become

$$(K^{ij} \theta_{,j})_{,i} + \rho s = 0. \quad (36)$$

- Recalling the assumptions of
 (e) thermal isotropy ($\bar{K} = K\bar{g}$) and
 (f) spherical symmetry,

and introducing the new assumption of

- (g) thermal homogeneity (K is a constant),
 causes Eq. (36) to become

$$\frac{1}{R^2} \frac{d}{dR} \left(R^2 \frac{d\theta}{dR} \right) + \frac{\rho s}{K} = 0 \quad . \quad (37)$$

In addition to the seven assumptions above, it was also assumed that

- (h) $K = {}_1K$ and $\rho s = Q$ (where Q is a constant) in the $0 \leq R < {}_1A$ region, and

- (i) $K = {}_2K$ and $\rho s = 0$ in the ${}_1A < R$ region.

The solution to Eq. (37), consistent with assumptions h and i, is given by⁸

$$\theta = Q \left[\left({}_1A \right)^2 - R^2 + 2 \left({}_1A \right)^2 \left(\frac{{}_1K}{{}_2K} \right) \right] / 6 \left({}_1K \right) \text{ in } 0 \leq R < {}_1A$$

and

$$\theta = Q \left({}_1A \right)^3 / 3 \left({}_2K \right) R \text{ in } {}_1A < R. \quad (38)$$

The temperature profile, defined by Eq. (38), is characterized by continuity of θ across Σ . However, $\text{grad}\theta$ is discontinuous unless ${}_1K = {}_2K$. Note that this first-generation model contains no provisions for convective or radiative energy transfer.

The constitutive coefficients \underline{B} , \underline{C} , \underline{D} , \underline{F} , \underline{G} , \underline{H} , ${}_1K$, and ${}_2K$ are essential to this first-generation model. No restrictions were placed on \underline{B} , \underline{C} , \underline{D} , ${}_1K$, and ${}_2K$, and the only restriction placed on \underline{F} , \underline{G} , and \underline{H} was that $\Sigma \underline{W} = \underline{0}$. There are restrictions, however, that should be placed on all but \underline{B} . These restrictions are a result of the requirement that the entropy inequality be satisfied.

Unfortunately, it is impossible to guarantee satisfaction of the entropy inequality by restricting the range of values occupied by coefficients in linear constitutive equations. Therefore, any restrictions placed on \underline{C} , \underline{D} , \underline{F} , \underline{G} , \underline{H} , ${}_1K$, and ${}_2K$ may be necessary, but they can never be sufficient.⁵ For this reason and because of the lengthy calculation required to find these

constraints, we decided to use some of Miller's more tractable restrictions⁵

for a two-constituent, nonreacting mixture and to assume that ${}_1K > 0$, ${}_2K > 0$, $\underline{F}^{\ell} > 0$, $\underline{C}^r > 0$, and $\underline{D}^r > 0$.

IV. ANALYTICAL MODEL

By combining Eqs. (11), (25), and (26) and using the spherical symmetry assumption, we obtain

$$\frac{\partial \rho}{\partial t} + \frac{1}{R^2} \frac{\partial}{\partial R} \left(R^2 \frac{\rho v}{\rho v} \right) = -\lambda \frac{{}^{21} \rho}{{}^m \rho}, \quad (39)$$

$$\frac{\partial \rho}{\partial t} + \frac{1}{R^2} \frac{\partial}{\partial R} \left(R^2 \frac{\rho v}{\rho v} \right) = \frac{234}{238} \lambda \frac{{}^{21} \rho}{{}^m \rho}, \quad (40)$$

$$\frac{\partial \rho}{\partial t} + \frac{1}{R^2} \frac{\partial}{\partial R} \left(R^2 \frac{\rho v}{\rho v} \right) = \frac{4}{238} \lambda \frac{{}^{21} \rho}{{}^m \rho}, \quad (41)$$

$$\frac{\partial \rho}{\partial t} + \frac{1}{R^2} \frac{\partial}{\partial R} \left(R^2 \frac{\rho v}{\rho v} \right) = 0, \quad (42)$$

and

$$\frac{\partial \rho}{\partial t} + \frac{1}{R^2} \frac{\partial}{\partial R} \left(R^2 \frac{\rho v}{\rho v} \right) = 0, \quad (43)$$

where $\frac{{}^{21} \rho}{{}^m \rho} = \frac{{}^2 e^{-\lambda t}}{\chi + \frac{{}^1}{\chi e^{-\lambda t}} + \frac{{}^3}{\chi} + \frac{{}^4}{\chi} + \frac{{}^5}{\chi} + \frac{{}^6}{\chi}}$.

Combining Eqs. (12), (29), (32), (33), and (38) produces 3 \underline{n} equations (\underline{n} for each i). The 2 \underline{n} equations, which correspond to $i = 2$ and 3, reduce to $0 = 0$ because of the spherical symmetry assumption. The \underline{n} equations, which correspond to $i = 1$, can be expressed in a reasonably tractable form by defining the following quantities.

$$\underline{\Gamma}^r = -\frac{r r}{B \rho \theta} + \frac{1}{R^2} \sum_{\ell=1}^{\underline{n}} \left(\frac{r^{\ell}}{C} - \frac{2}{3} \frac{r^{\ell}}{D} \right) \frac{\partial}{\partial R} \left(R^2 \frac{\rho v}{\rho v} \right),$$

$$\underline{\Psi}^r = \sum_{\ell=1}^{\underline{n}} \frac{r^{\ell}}{2D} \frac{\partial \rho v}{\partial R},$$

and

$$\underline{\Omega} = \sum_{\ell=1}^n \frac{r^\ell}{2D} \frac{\underline{v}}{R} .$$

Using the assumptions that $\underline{b}^i = 0$ and $\underline{F} = \underline{F}$, we obtain

$$\begin{aligned} \frac{\partial}{\partial t} \left(\frac{11}{\rho v} \right) + \frac{1}{R^2} \frac{\partial}{\partial R} \left[R^2 \frac{1}{\rho} (\underline{v})^2 \right] - \frac{\partial}{\partial R} \left(\frac{1}{\Gamma} + \frac{1}{\Psi} \right) - \frac{2}{R} \left(\frac{1}{\Psi} - \frac{1}{\Omega} \right) = - \rho \underline{F} \left(\frac{1}{v} - \frac{2}{v} \right) \\ - \rho \underline{F} \left(\frac{1}{v} - \frac{3}{v} \right) - \rho \underline{F} \left(\frac{1}{v} - \frac{4}{v} \right) - \rho \underline{F} \left(\frac{1}{v} - \frac{5}{v} \right) - \rho \sum_{\ell=1}^n \frac{1}{G} \left(\frac{\partial \underline{\rho}}{\partial R} \right) - \rho \underline{H} \frac{d\theta}{dR} , \end{aligned} \quad (44)$$

$$\begin{aligned} \frac{\partial}{\partial t} \left(\frac{22}{\rho v} \right) + \frac{1}{R^2} \frac{\partial}{\partial R} \left[R^2 \frac{2}{\rho} (\underline{v})^2 \right] - \frac{\partial}{\partial R} \left(\frac{2}{\Gamma} + \frac{2}{\Psi} \right) - \frac{2}{R} \left(\frac{2}{\Psi} - \frac{2}{\Omega} \right) = - \rho \underline{F} \left(\frac{2}{v} - \frac{1}{v} \right) \\ - \rho \underline{F} \left(\frac{2}{v} - \frac{3}{v} \right) - \rho \underline{F} \left(\frac{2}{v} - \frac{4}{v} \right) - \rho \underline{F} \left(\frac{2}{v} - \frac{5}{v} \right) - \rho \sum_{\ell=1}^n \frac{2}{G} \left(\frac{\partial \underline{\rho}}{\partial R} \right) - \rho \underline{H} \frac{d\theta}{dR} , \end{aligned} \quad (45)$$

$$\begin{aligned} \frac{\partial}{\partial t} \left(\frac{33}{\rho v} \right) + \frac{1}{R^2} \frac{\partial}{\partial R} \left[R^2 \frac{3}{\rho} (\underline{v})^2 \right] - \frac{\partial}{\partial R} \left(\frac{3}{\Gamma} + \frac{3}{\Psi} \right) - \frac{2}{R} \left(\frac{3}{\Psi} - \frac{3}{\Omega} \right) = - \rho \underline{F} \left(\frac{3}{v} - \frac{1}{v} \right) \\ - \rho \underline{F} \left(\frac{3}{v} - \frac{2}{v} \right) - \rho \underline{F} \left(\frac{3}{v} - \frac{4}{v} \right) - \rho \underline{F} \left(\frac{3}{v} - \frac{5}{v} \right) - \rho \sum_{\ell=1}^n \frac{3}{G} \left(\frac{\partial \underline{\rho}}{\partial R} \right) - \rho \underline{H} \frac{d\theta}{dR} , \end{aligned} \quad (46)$$

$$\begin{aligned} \frac{\partial}{\partial t} \left(\frac{44}{\rho v} \right) + \frac{1}{R^2} \frac{\partial}{\partial R} \left[R^2 \frac{4}{\rho} (\underline{v})^2 \right] - \frac{\partial}{\partial R} \left(\frac{4}{\Gamma} + \frac{4}{\Psi} \right) - \frac{2}{R} \left(\frac{4}{\Psi} - \frac{4}{\Omega} \right) = - \rho \underline{F} \left(\frac{4}{v} - \frac{1}{v} \right) \\ - \rho \underline{F} \left(\frac{4}{v} - \frac{2}{v} \right) - \rho \underline{F} \left(\frac{4}{v} - \frac{3}{v} \right) - \rho \underline{F} \left(\frac{4}{v} - \frac{5}{v} \right) - \rho \sum_{\ell=1}^n \frac{4}{G} \left(\frac{\partial \underline{\rho}}{\partial R} \right) - \rho \underline{H} \frac{d\theta}{dR} , \end{aligned} \quad (47)$$

and

$$\begin{aligned}
& \frac{\partial}{\partial t} \left(\frac{55}{\rho v} \right) + \frac{1}{R^2} \frac{\partial}{\partial R} \left[R^2 \frac{55}{\rho} (v)^2 \right] - \frac{\partial}{\partial R} \left(\frac{5}{\Gamma} + \frac{5}{\Psi} \right) - \frac{2}{R} \left(\frac{5}{\Psi} - \frac{5}{\Omega} \right) = -\rho \frac{15}{F} \left(\frac{5}{v} - \frac{1}{v} \right) \\
& -\rho \frac{25}{F} \left(\frac{5}{v} - \frac{2}{v} \right) - \rho \frac{35}{F} \left(\frac{5}{v} - \frac{3}{v} \right) - \rho \frac{45}{F} \left(\frac{5}{v} - \frac{4}{v} \right) + \rho \frac{\partial \rho}{\partial R} \sum_{r=1}^4 \frac{r_1}{G} + \rho \frac{\partial \rho}{\partial R} \sum_{r=1}^4 \frac{r_2}{G} \\
& + \rho \frac{\partial \rho}{\partial R} \sum_{r=1}^3 \frac{r_3}{G} + \rho \frac{\partial \rho}{\partial R} \sum_{r=1}^4 \frac{r_4}{G} + \rho \frac{\partial \rho}{\partial R} \sum_{r=1}^5 \frac{r_5}{G} + \rho \frac{d\theta}{dR} \sum_{r=1}^4 \frac{r}{H} , \tag{48}
\end{aligned}$$

where θ is defined by Eq. (38).

Equations (39)-(43) and (44)-(48) express the balance of mass and balance of radial linear momentum, respectively, for each group of constituents, at regular points of the mixture. These ten equations, which contain the ten unknowns $\rho_r(R,t)$ and $v_r(R,t)$, must be satisfied at each point in the $0 \leq R < {}_1A$ and ${}_1A < R \leq {}_2A$ regions. The appropriate boundary conditions are $\frac{r}{v}(0,t) = \frac{r}{v}({}_2A,t) = 0$.

Equation (19) is repeated here, for reference purposes, as Eq. (49).

$$\left[\left[\frac{r}{\rho} \frac{r}{v} \right] \right] = 0 \quad . \tag{49}$$

Combining Eqs. (20), (21), (22), and (29) produces $3\underline{n}$ equations (\underline{n} for each i). The $2\underline{n}$ equations, which correspond to $i = 2$ and 3 , reduce to $0 = 0$ because of the spherical symmetry assumption. The \underline{n} equations, which correspond to $i = 1$, are

$$\left[\left[\frac{r}{\rho} \frac{r}{(v)}^2 - \left(\frac{r}{\Gamma} + \frac{r}{\Psi} \right) \right] \right] = 0. \tag{50}$$

Equations (49) and (50) express the balance of mass and balance of radial linear momentum, respectively, for each group of constituents, at the surface Σ .

Equations (39)-(50) comprise the analytical model that was developed to simulate multiconstituent diffusion, helium generation, and helium release. The numerical integration of the model is discussed in Sec. V.

This first-generation model is consistent with the fundamental requirement that balance of mass, linear momentum, angular momentum, and energy be achieved

for the total mixture at all points of the $0 \leq R \leq 2A$ region.

- (a) Because mass is balanced for each group of constituents in the $0 \leq R \leq 2A$ region, then mass is also balanced for the total mixture in that region.
- (b) Because linear momentum is balanced for each group of constituents in the $0 \leq R \leq 2A$ region, then linear momentum is also balanced for the total mixture in that region.
- (c) Equation (13) is automatically satisfied because each \bar{T}^r is symmetrical. It follows, from Eq. (9.3), that \bar{T} is symmetrical. The symmetry of \bar{T} ensures that angular momentum is balanced for the total mixture at all regular points. At Σ , angular momentum is balanced for the total mixture because linear momentum is balanced for the total mixture.⁹
- (d) Energy is balanced for the total mixture at all regular points because Eq. (38) was obtained from Eq. (35). At Σ , energy is balanced for the total mixture because Eq. (24) is automatically satisfied by $q = K \frac{d\theta}{dR}$.

V. NUMERICAL INTEGRATION

I developed a semi-implicit, finite difference FORTRAN code to integrate Eqs. (39)-(50) numerically. The computer program now accepts only constant values for the constitutive coefficients \underline{B} , \underline{C}^l , \underline{D}^l , \underline{F}^l , \underline{G}^l , and \underline{H} , although for a given coefficient, a different constant may be used in the $0 \leq R < 1A$ region than is used in the $1A < R \leq 2A$ region. This constant coefficient restriction cannot be justified by constitutive theory. According to constitutive theory, each coefficient can be functionally dependent on $\bar{\rho}$ and θ (Ref. 5). Unfortunately, the nature of the functions $\underline{B}(\bar{\rho}, \theta)$, $\underline{C}^l(\bar{\rho}, \theta)$, $\underline{D}^l(\bar{\rho}, \theta)$, $\underline{F}^l(\bar{\rho}, \theta)$, $\underline{G}^l(\bar{\rho}, \theta)$, and $\underline{H}(\bar{\rho}, \theta)$ is unknown. One is tempted to use some type of Arrhenius temperature dependence for certain coefficients as is so often done for the diffusivity in Fick's Law, but the validity of such an assumption has not been demonstrated.

VI. CONCLUSIONS AND DISCUSSION

A. Helium

Figure 1 shows the existing data on helium release obtained from actual heat source spheres. The data were obtained from two spheres (SPO-30 and SPO-39) by maintaining their surface temperatures at 1308 and 1278 K, respectively, and monitoring release rate with a helium leak detector. Before testing, the two

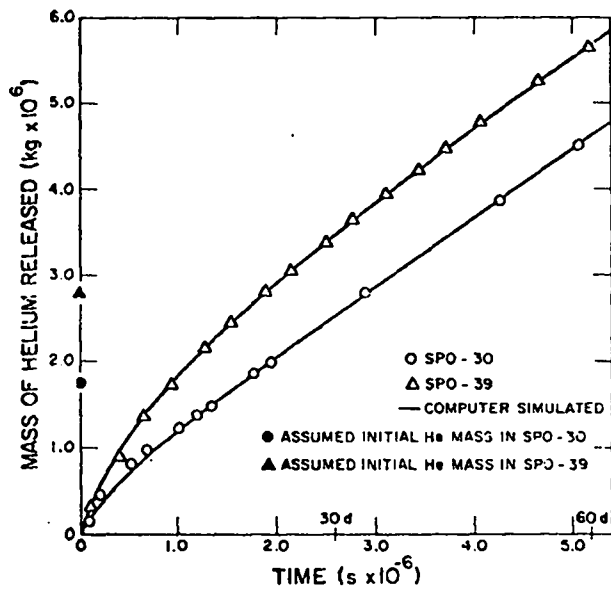


Fig. 1.
Helium release.

spheres were cooled to 800-825 K for several days. At such low temperatures, helium release is severely retarded and significant amounts of helium accumulate within the sphere. Figure 1 shows that more helium was stored in SPO-39 than in SPO-30. This is a reasonable finding considering that SPO-39 was allowed to "incubate" at 800-825 K for about 400 h longer than SPO-30.

Each sphere, which consisted nominally of 0.253 kg PuO₂, had a radius of 0.0186 m. Before obtaining the helium release data shown in Fig. 1, the spheres were used for iridium compatibility and helium vent evaluations.

The Fig. 1 data were obtained using a Veeco leak detector attached to a vacuum-tight furnace chamber. The solid lines represent a computer-simulated helium release. In both cases, the helium distribution within the sphere was presumed to be uniform at $t = 0$. The two curves were generated without changing any of the constitutive coefficients. The only input parameter changed was the initial helium density within the heat source sphere. The helium masses that correspond to these initial densities are indicated along the ordinate.

We will not itemize the B , C , D , F , G , and H values used to generate the solid lines in Fig. 1 because (1) no independent determination of constitutive coefficients was made and (2) a reasonable data fit may be obtained by using more than one set of input parameters. Although the worth of the model is certainly susceptible to criticism on these grounds, the fit in Fig. 1 is undeniably good.

B. Trace Impurity

All the existing data on trace impurity mass transport are contained in Table III. The data, accurate to within $\pm 20\%$, were obtained from SPO-40 by maintaining its surface temperature at 1713 K for 18 293 h; obtaining a radial section; dividing this radial section into four parts; and analyzing each part for calcium, silicon, and aluminum by emission spectroscopy.

It is unlikely that the trace impurity distributions given in Table III were characteristic of SPO-40 during manufacture. Moreover, if all three trace

TABLE III
TRACE IMPURITY CONTENT

<u>Specimen</u>	<u>Calcium (ppm)</u>	<u>Silicon (ppm)</u>	<u>Aluminum (ppm)</u>	
1	250	140	270	Surface
2	250	150	60	↑
3	250	100	100	↓
4	500	90	120	Center

impurities were uniformly distributed immediately after sintering, then the concentration gradient could not have been the dominant "driving force" for redistribution.

It appears that the calcium in SPO-40 migrated toward $R = 0$, whereas the aluminum and silicon migrated toward Σ . Because it did not occur to me, during development of the model, that two different cationic trace impurities might move with different velocity distributions, all cationic trace impurities were "lumped together" as one constituent. Consequently, the model cannot simulate the mass transport of more than one trace impurity at a time.

Because calcium is the dominant trace impurity in heat source spheres, we attempted to reproduce the general shape of the calcium density profile, indicated by the data in Table III, while simultaneously simulating helium release. Figures 2-5 represent computer-simulated radial density profiles for 5, 50, 500, and 5000 h, respectively. Each curve was generated using the same input parameters used to generate the lower helium release curve in Fig. 1. Trace impurity density, at $t = 0$, was set equal to 2.5 kg/m^3 throughout the heat source sphere. Figures 2-5 show that the trace impurity is migrating toward the center of the sphere. However, each curve is either flat or concave downward near $R = 0$. Even after 10 000 h of simulated mass transport, the curvature centers continue to lie below the curve in this region. It is my opinion that at least some of the constitutive coefficients must be allowed to vary with temperature to generate the type of calcium density profile indicated by the Table III data. This is an unexpected conclusion because the temperature at the center of a sphere is only 100 K higher than the temperature at its surface.

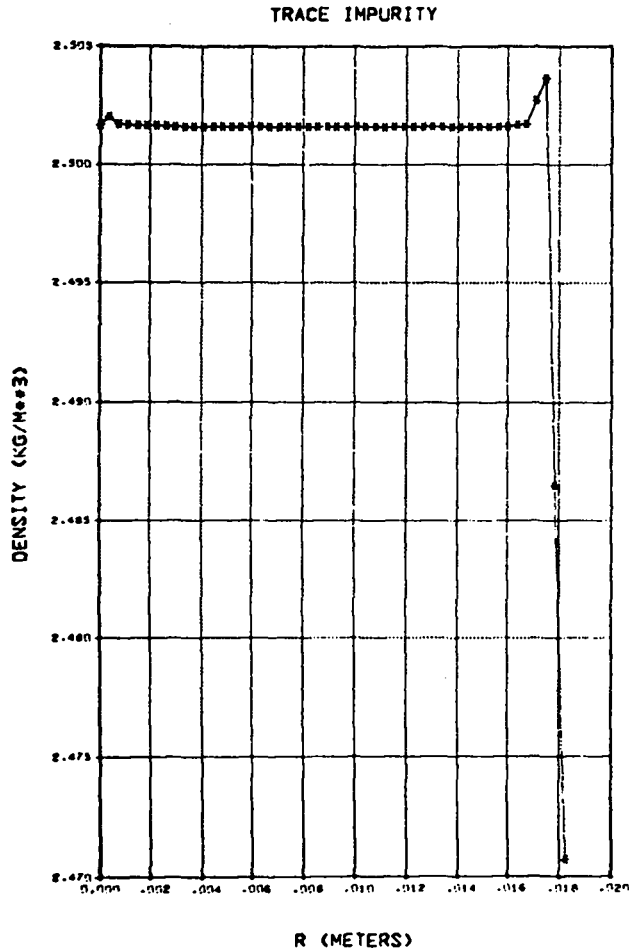


Fig. 2.

Computer-simulated radial density profile for calcium at 5 h.

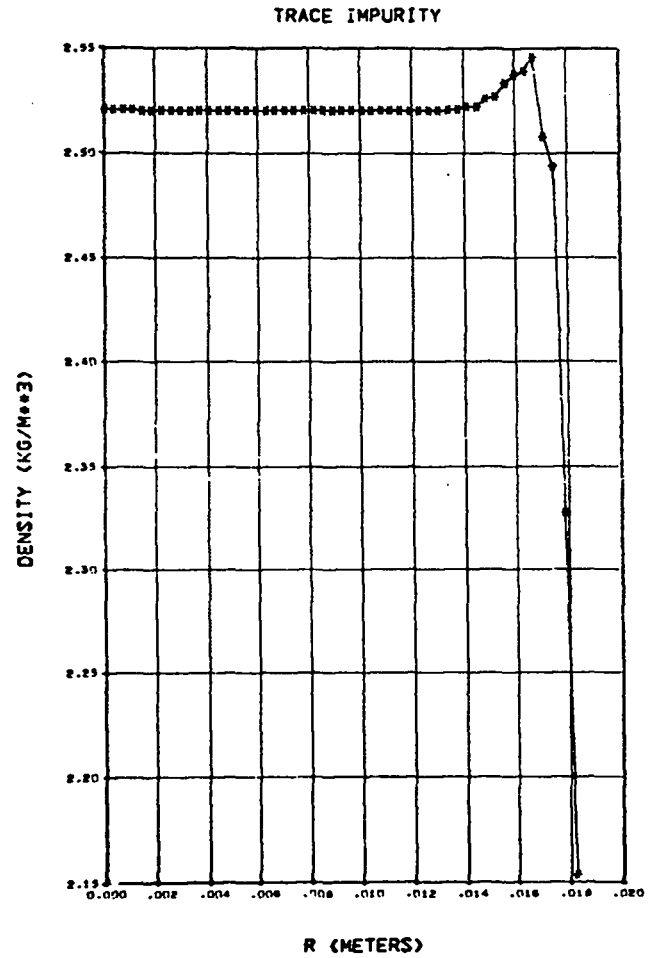


Fig. 3.

Computer-simulated radial density profile for calcium at 50 h.

C. Plutonium-Uranium-Oxygen

There is no experimental information available on the mass transport of plutonium, uranium, or oxygen in heat source spheres. Emission spectroscopy is not a satisfactory technique. The electron microprobe can detect these elements, but it cannot detect small density changes during a radial scan. Other analytical techniques, such as spectrophotometry, x-ray fluorescence, and perhaps ion probe analysis, will be evaluated in the future.

For several years, it has been known that the various constituents that make up hypostoichiometric (U,Pu) oxide reactor fuel rods tend to redistribute by thermal diffusion.¹⁰⁻¹⁴ For example, plutonium tends to migrate toward the higher temperature (~2700 K) center axis of a rod, whereas uranium and oxygen tend to migrate toward the lower temperature (~1300 K) cylindrical surface. We can expect

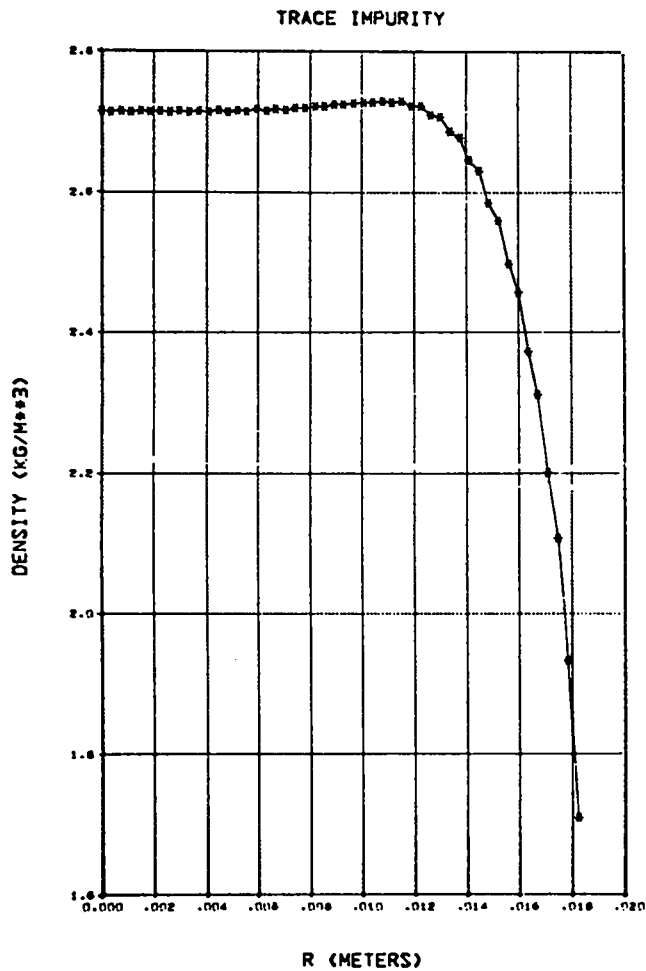


Fig. 4.
Computer-simulated radial density profile for calcium at 500 h.

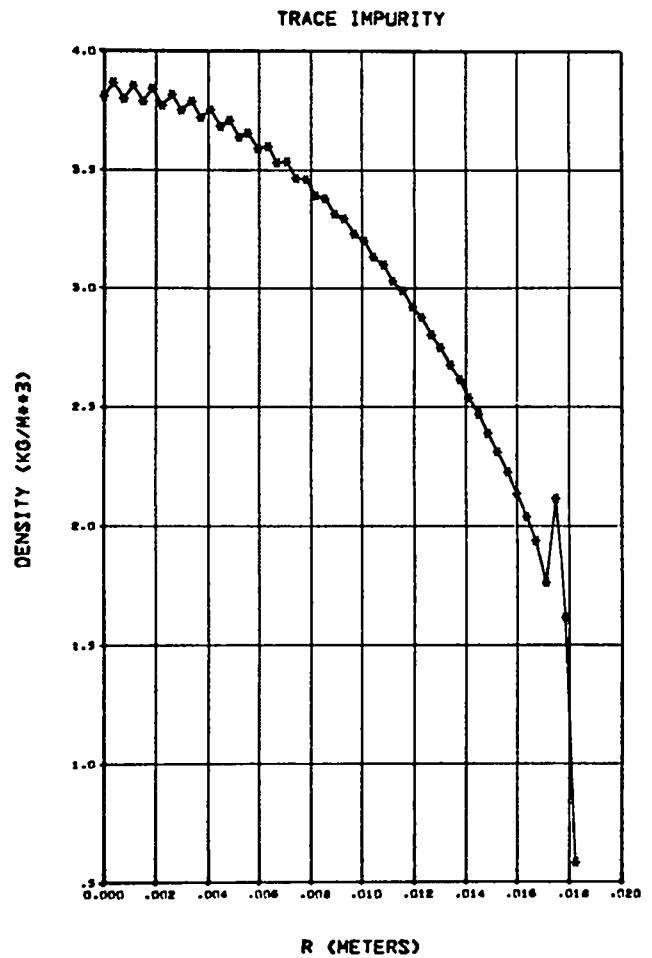


Fig. 5.
Computer-simulated radial density profile for calcium at 5000 h.

the same type of thermally induced mass transport to occur in a heat source sphere--the only difference being one of degree rather than kind.

Figures 6-8 show the computer-simulated radial density profiles, at 500 h, for plutonium, uranium, and oxygen, respectively. Each curve was generated using the same input parameters used to generate the lower helium release curve in Fig. 1. Plutonium, uranium, and oxygen densities, at $t = 0$, were set equal to 8400, 84, and 1130 kg/m^3 , respectively, throughout the heat source sphere. The degree of agreement between the computer-simulated density profiles and actual density profiles cannot be determined without experimental data. The direction of transport, indicated by each figure, is probably correct. However, the model may not be able to simulate the actual shape of the radial density profiles without using temperature-dependent constitutive coefficients.

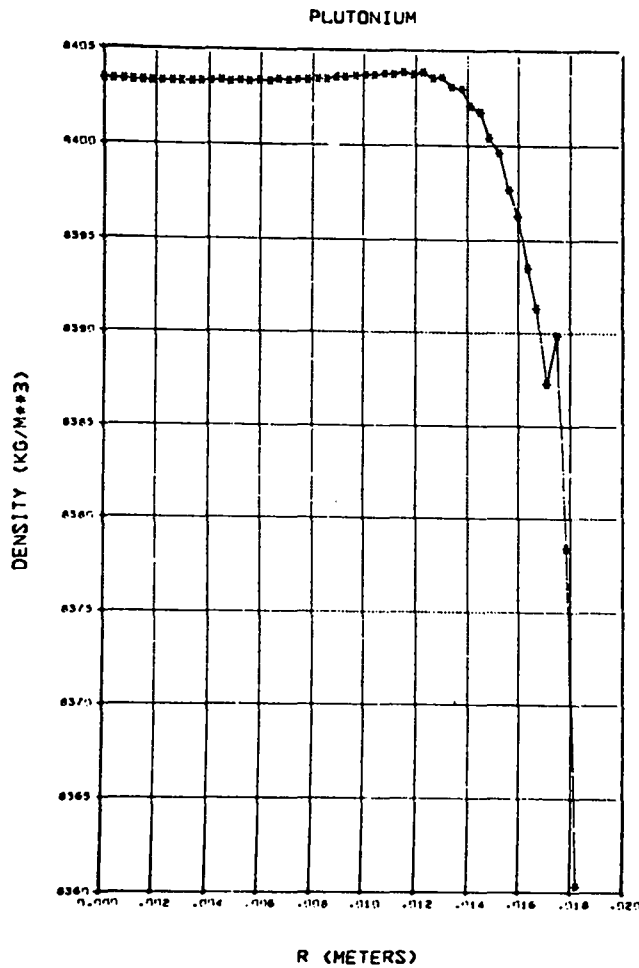


Fig. 6.
Computer-simulated radial density profile for plutonium at 500 h.

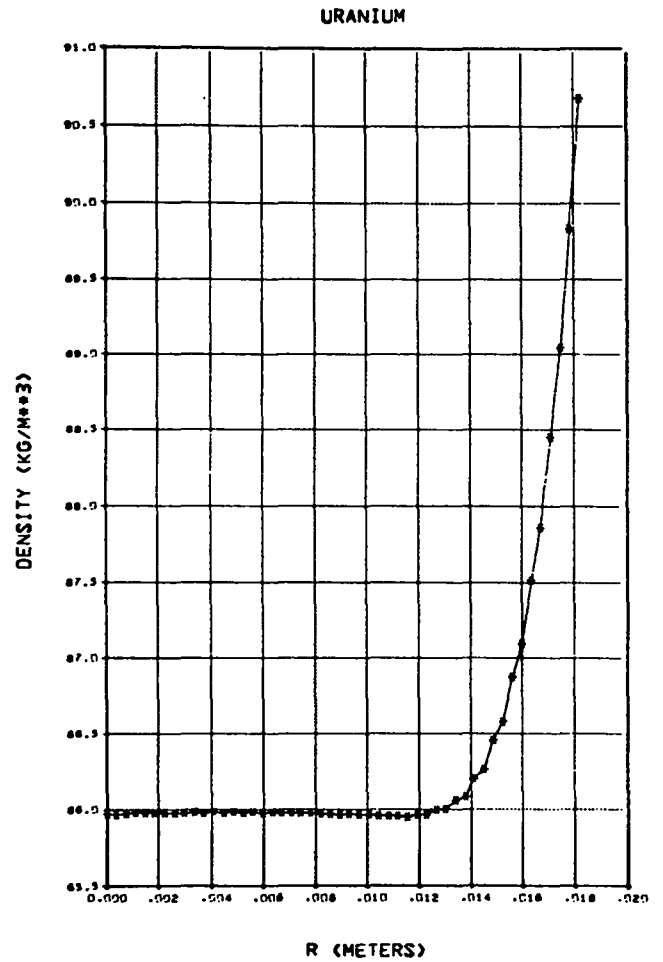


Fig. 7.
Computer-simulated radial density profile for uranium at 500 h.

We have established that this first-generation model, which represents the first attempt to simulate multiconstituent mass transport using Truesdell's theory of mixtures, can adequately simulate helium generation and helium release. We feel that with some minor additions, such as incorporation of two more constituents and explicit use of temperature-dependent constitutive coefficients, the model will also be able to simulate multiconstituent diffusion.

This model was based on so many assumptions, some of which are so restrictive, that the model might have proved to be totally inadequate. For example, all grain boundaries were ignored although they probably provide a preferred path for helium diffusion. One of the weakest assumptions is that a heat source sphere is a mixture of linearly viscous fluids. If the internal helium generation were to produce a significant stress on the (U,Pu) oxide lattice, Eq. (29) could not

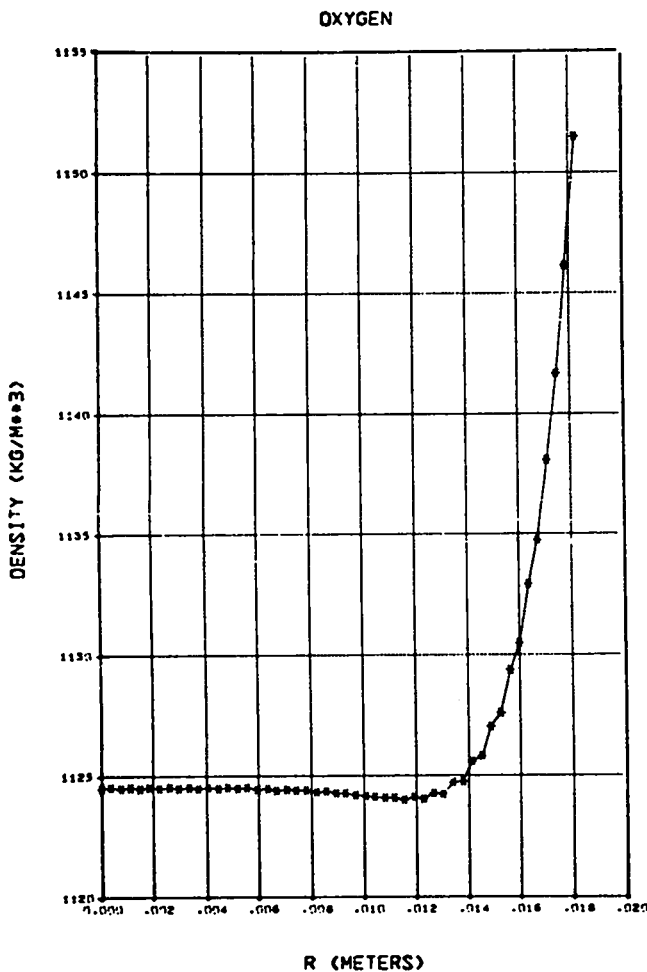


Fig. 8.
Computer-simulated radial density profile for oxygen at 500 h.

describe this stress. Miller's constitutive equation for \bar{T} was used only because comparable equations for nonfluid mixtures have not been developed. However, the use of Eq. (29) for helium may not be too unreasonable. Note that all the computer simulations presented here were obtained with \bar{T} set equal to $\bar{0}$ for $r = 1, 2, 4,$ and 5 .

Further progress, in using Truesdell's theory of mixtures to model the class of phenomena discussed in this report, awaits developments in three areas:

(a) Experimental determination of constitutive coefficients--how does one measure \underline{F} , \underline{G} and \underline{H} ?

(b) Theoretical prediction regarding the variation of constitutive coefficients with temperature--is it reasonable to let $\underline{H}(\rho, \theta) = [\underline{H}_0(\rho)]e^{-\Phi/\theta}$ where Φ is a constant?

(c) Theoretical prediction regarding constitutive equations for \bar{T} (and \bar{W}) applicable to crystalline solid mixtures.

The work presented in this report should be regarded as merely a first step. The ultimate goals of the program are to develop

- (a) A model that can simulate (1) diffusion of plutonium, uranium, helium, oxygen, calcium, aluminum, and silicon within a heat source (2) generation of helium within a heat source, and (3) release of plutonium, uranium, helium, oxygen, calcium, aluminum, and silicon from the surface of heat source material into the surrounding environment;
- (b) Computer codes that can produce numerical solutions for various heat source geometries; and
- (c) Measured constitutive coefficient values over a range of θ (and possibly $\underline{\rho}$).

The next steps toward these goals will be to rework this first-generation model with the objective of incorporating two more constituents and certain other features intended to extend its generality; rewrite the computer code in accordance with the revised model with explicit provisions for variable constitutive coefficients; obtain more data regarding the radial density profiles of various constituents as functions of time and temperature; and obtain at least rudimentary data concerning sublimation of trace impurities.

Further steps will depend on how much progress has been made in the use of Truesdell's theory of mixtures. Problems, such as experimental determination of constitutive coefficients, theoretical variation of constitutive coefficients with temperature, and theoretical determination of constitutive equations for crystalline solid mixtures, have not been seriously studied. The solutions to such problems are of real interest only to those persons involved in the practical application of Truesdell's theory, which has not been regarded by the materials science community as a viable alternative to nonequilibrium thermodynamics. However, this report has demonstrated that Truesdell's theory is a viable alternative. Furthermore, those persons who have been unsuccessful in understanding the fundamental axioms of nonequilibrium thermodynamics may find that Truesdell's theory is a very satisfactory alternative.

REFERENCES

1. C. Truesdell, "Mechanical Basis of Diffusion," *J. Chem. Phys.* 37, 2336-2344 (1962).
2. L. A. Girifalco, "Diffusion in Non-Uniform Crystals," *Mater. Sci. Eng.* 9, 61-79 (1972).
3. S. R. De Groot and P. Mazur, Non-Equilibrium Thermodynamics (North-Holland, Amsterdam, 1962).
4. C. Truesdell, Rational Thermodynamics (McGraw-Hill, New York, 1969), Chapters 5 and 7.
5. I. Müller, "A Thermodynamic Theory of Mixtures of Fluids," *Arch. Ration. Mech. Anal.* 28, 1-39 (1968).
6. R. Benach and I. Müller, "Thermodynamics and the Description of Magnetizable Dielectric Mixtures of Fluids," *Arch. Ration. Mech. Anal.* 53, 312-346 (1973-74).
7. P. D. Kelley, "A Reacting Continuum," *Int. J. Eng. Sci.* 2, 129-153 (1964).

8. H. S. Carslaw and J. C. Jaeger, Conduction of Heat in Solids (Oxford University Press, London, 1959), p. 232.
9. C. Truesdell and R. Toupin, "The Classical Field Theories," in Flügge's Encyclopedia of Physics (Springer-Verlag, Berlin, 1960), Vol. 3, Part 1, p. 547.
10. E. A. Aitken, "Thermal Diffusion in Closed Oxide Fuel Systems," J. Nucl. Mater. 30, 62-73 (1969).
11. M. Bober, C. Sari, and G. Schumacher, "Redistribution of Plutonium and Uranium in Mixed (U,Pu) Oxide Fuel Materials in a Thermal Gradient," J. Nucl. Mater. 39, 265-284 (1971).
12. I. Johnson, C. E. Johnson, C. E. Crouthamel, and C. A. Seils, "Oxygen Potential of Irradiated Urania-Plutonia Fuel Pins," J. Nucl. Mater. 48, 21-34 (1973).
13. M. Bober and G. Schumacher, "Considerations on the Oxygen Distribution in Hypostoichiometric Mixed Oxide Fuel Pins," J. Nucl. Mater. 49, 322-324 (1973-74).
14. C. Sari and G. Schumacher, "Thermal Diffusion of Oxygen in PuO_{2-y} ," Nucl. Technol. 28, 256-260 (1976).